Journal of Solid State Chemistry **150,** 399–403 (2000)
doi:10.1006/jssc.1999.8613, available online at http://www.idealibrary.com on IDEAL®

Phase Transition in Cs_2KMnF_6: Crystal Structures of Low- and High-Temperature Modifications

Y. Xu, S. Carlson, A. Sjödin, and R. Norrestam[1]

Structural Chemistry, Arrhenius Laboratory, Stockholm University, S-106 91 Stockholm, Sweden

Received October 20, 1999; accepted December 13, 1999

Crystalline Cs_2KMnF_6, when prepared below 500°C, adopts a tetragonal elpasolite structure type. Differential scanning calorimetric investigations indicated that Cs_2KMnF_6 undergoes a phase transition from the low-temperature tetragonal phase (LT) to a high-temperature phase (HT) at about 530°C. Single crystals of the new HT phase could be obtained by annealing a crystalline LT specimen at 600°C followed by rapid quenching to room temperature. In the present study the structures of both phases have been studied by single-crystal X-ray diffraction techniques. The LT phase has the tetragonal space group symmetry *I*4/*mmm*, with unit-cell parameters $a = 6.319(1)$ ($a \cdot \sqrt{2} = 8.936$) and $c = 9.257(2)$ Å, and $Z = 2$. The HT phase has the cubic symmetry *Fm3m*, with the cell parameter $a = 9.067$ Å and $Z = 4$. Structural models of the LT and HT phases have been refined vs collected single-crystal X-ray reflection data to *R* values of 0.034 and 0.022, respectively. The uneven Mn–F bond distance distribution in the LT form, four bonds of 1.860(6) two of 2.034(9) Å, are typical for an octahedrally coordinated high-spin Mn^{3+} ion affected by Jahn–Teller effects. Due to symmetry constraints, all six octahedral Mn–F bonds in the HT form are equal to 1.931(5) Å. However, the mean square atomic displacement parameters of the fluorine atoms increases significantly from about 0.022 Å² for the LT phase to 0.042 Å² for the HT phase. The increased displacement parameters indicate that the phase transition from the LT to the HT form is associated with a directional disorder of the Jahn–Teller distortions around the Mn^{3+} ions.

Key Words: **single crystal study; Mn^{3+} elpasolite; phase transition.**

INTRODUCTION

The crystal structure of Cs_2KMnF_6 has been previously reported by Schneider and Hoppe (1) to have a tetragonal elpasolite structure of the K_2NaMnF_6 type (cf. Knox (2)), with $F4/mmm$ space group symmetry. This previous study, which was based exclusively on X-ray powder diffraction data from a polycrystalline specimen, gave the tetragonal unit cell parameters $a = 8.933(5)$ and $c = 9.265(5)$ Å.

[1] To whom correspondence should be addressed.

The elpasolite structure can be considered (cf. Fig. 1) as a lower symmetry variant of the cryolite structure. Accordingly, elpasolite is related to the perovskite-type structure, and the general features of its structure are a three-dimensional array of corner-connected $(K,Mn)F_6$ octahedra with the Cs atoms in the cuboctahedral interstices formed between the $(K,Mn)F_6$ octahedra. The Goldschmidt "tolerance factor," $t = d_{A\text{–}F}/\sqrt{2}d_{B\text{–}X}$, for perovskites (see, e.g., Hyde and Andersson (3)) becomes about 0.97 for A_2BMF_6 with the ionic radii estimates given by Shannon (4). This value is well within the region for expected cubic symmetry (0.89–1.00). A cubic symmetry is also observed for ideal elpasolites like K_2NaAlF_6. However Cs_2KMnF_6 contain Mn^{3+} ions with d^4 electron configurations. In fluorides and oxides the Mn^{3+} ions are generally in a high-spin state. This will imply Jahn–Teller type of distortions on the MnF_6 coordination octahedra. As a consequence, an axial ordering of the distortions of the MnF_6 octahedra might lower the space group symmetry, from cubic for an ideal elpasolite like K_2NaAlF_6, to tetragonal for Cs_2KMnF_6. The magnitudes of the distortions are however limited and a disorder of the distortion directions might be anticipated to occur, at least at elevated temperatures. By such a disorder the expected symmetry can increase from tetragonal to cubic.

As anticipated (cf. discussion above), differential scanning calorimetry performed within the present study indicated that Cs_2KMnF_6 undergoes a phase transition at about 530°C to a high-temperature phase (HT) later shown to be cubic. From collected single-crystal X-ray diffraction data, crystal structure models of both the low temperature (LT) and the HT phases, have been refined. The studies of Mn^{3+} containing elpasolite structures is part of a research project concerning structural studies at different pressures/temperatures of transition metal fluorides, particularly those containing Jahn–Teller distortions.

EXPERIMENTAL

Synthesis

The LT phase was synthesized by heating a stoichiometric mixture with the composition $2CsF + KF + MnF_3$ at

0022-4596/00 $35.00

elevated pressure. Dried CsF (Aldrich, no. 25.571-8), KF (Merck, no. 1.04994), and MnF_3 (Aldrich, no. 33.929-6) were mixed together in an agate mortar in a glove box filled with argon. The mixture was put into a gold ampule, which was sealed and inserted into a stainless-steel container. The steel container was filled with water, heated up to 520°C at an external pressure of 2.5 kbar, and kept under these conditions for 5 h. The steel container with the sample was then allowed to cool slowly (15–20 h) from 520°C to room temperature.

The HT phase was obtained by rapidly quenching a previously synthesized LT specimen from a temperature well above the observed transition point (≈ 530°C). The LT specimen was put into a platinum tube, which was sealed and inserted into a quartz ampule. The quartz ampule was then evacuated, sealed and heated to 600°C during 24 h, and finally quenched in cold water.

X-Ray Studies

The synthetic products were examined by Guinier X-ray powder techniques. The powder diffraction pattern collected for the LT phase was in agreement with that previously published (Schneider and Hoppe (1)) and could thus be indexed with a nonconventional *F*-centered tetragonal unit cell with the dimensions $a = 8.9294(4)$, $c = 9.2638(4)$ Å ($V = 738.64(6)$ Å^3). For the corresponding conventional *I*-centered tetragonal space group symmetry utilized throughout the present study, the unit-cell dimensions are $a = a/\sqrt{2} = 6.3140(3)$, $c = 9.2638(4)$ Å ($V = 369.32(3)$ Å^3). The cell dimensions for the HT phase of a *F*-centered cubic cell became $a = 9.0569(5)$ Å ($V = 742.90(7)$ Å^3).

Single-crystal photographic techniques (de Jong and precession techniques) were utilized to find suitable crystals for the single-crystal diffraction studies. Crystal X-ray intensity data were collected with a four-circle diffractometer (Siemens *P4/RA*) equipped with a high-speed scintillation detector (Siemens *FSD*), using graphite monochromatized Mo$K\alpha$ radiation ($\lambda = 0.71073$ Å) from a rotating anode generator (Siemens M18XHF). The generator was operated at 5.0 kW (50 kV and 100 mA) for a filament size of 0.3×3 mm. A beam collimator with an inner diameter of 0.3 mm was used. The collected X-ray diffraction data were corrected for Lorenz and polarization effects. A numerical absorption correction was performed, using the STADI4 software package (STOE 1997).

The X-ray diffraction intensity data collected for the LT phase were consistent with the tetragonal space group symmetry *I*4/*mmm*. The unit-cell parameters $a = 6.319(1)$, $c = 9.257(2)$ Å ($V = 369.6(1)$ Å^3) were determined by refining them against the setting angles of 12 reflections, well centered and well distributed in the reciprocal space. These cell parameters are in agreement with the unit-cell parameters $a = 8.933(5)$ ($a/\sqrt{2} = 6.317(3)$ Å) and $c = 9.265(5)$ Å previously reported by Schneider and Hoppe (1), when the space group symmetry is alternatively described with the nonconventional space group symmetry *F*4/*mmm*. The refinements (cf. Table 1) of a structure model, checked by an interpretation of the Patterson function, using 11 parameters converged smoothly for 121 observed unique reflections to an *R* value of 0.034 ($wR = 0.035$). Anisotropic thermal displacement parameters were allowed for the Cs, Mn, and K atoms, while the F atoms were kept isotropic in the final refinements. When allowing anisotropic displacement parameters also for the F atoms, the values obtained did not deviate significantly from an isotropic model.

The intensity data collected for the HT phase indicated a cubic *Fm*3*m* space group symmetry. Refining the cell parameters against 12 well-centered reflections gave $a = 9.067(1)$ Å ($V = 745.4(2)$ Å^3). Compared to the LT phase, the volume increase for the HT phase is 2.0%. The refinements (cf. Table 1) of a structure model using 7 parameters versus 98 uniquely observed reflections converged to an *R* value of 0.022 ($wR = 0.028$). The constraints, imposed by the cubic symmetry of the structure, allows only anisotropic displacement parameters for the F atoms. Refinements of models, where the occupation factors of the two alkali metal positions were varied, gave occupation factors not significantly different from 1.00.

All structure refinements were made using the SHELXTL PC software package (5), using neutral atomic scattering factors from "International Tables of Crystallography" (6). Geometric calculations were performed with the program PLATON (7) and the structure diagrams were made using the program ATOMS (8). Further experimental details for the X-ray data collections and structure refinements are shown in Table 1, and the obtained structural parameter values are given in Table 2.

DSC Studies

Differential scanning calorimetry (DSC) measurements, using a differential scanning calorimeter (Perkin–Elmer DSC-2C), were performed on the LT phase of Cs_2KMnF_6 under argon atmosphere. In the temperature range from 420 to 620°C a small exothermic peak was observed at about 530°C when increasing the temperature (10°C/min), and a small endothermic dip at 525°C when decreasing the temperature. The different transition temperatures observed are probably due to a hysteresis effect, as is common for, e.g., first-order transitions. A Guinier powder diffraction pattern for the specimen after the DSC experiment indicates that the major phase was the LT phase, but traces of the HT phase were still observable. Thus, according to the DSC experiments the transition is not complete or the quenching procedure is not entirely effective.

TABLE 1
Experimental Details (esds in Parentheses) for the Structure Determinations of Low-Temperature (LT) and High-Temperature (HT) Phases of Cs_2KMnF_6

	LT-Cs_2KMnF_6	HT-Cs_2KMnF_6
Space group symmetry	$I4/mmm$	$Fm3m$
Formula units per unit cell, Z	2	4
Unit cell dimensions (Å), $T = 293$ K	$a = 6.3190(10)$, $c = 9.257(2)$	$a = 9.0670(10)$
Unit cell volume, V(Å^3)	369.63(11)	745.40(14)
Calculated density, d_X (g·cm^{-3})	4.258	4.222
Intensity data collection:	ω–2θ scan	
Maximum $\sin(\theta)/\lambda$(Å^{-1})	0.73	0.98
Collected reflections	568	827
Unique reflections	178	189
Observed reflections ($\|F\| \geq 3\cdot\sigma_F$)	121	98
Absorption correction	Numerical integration	
Crystal size (μm^3)	$60 \times 90 \times 120$	$150 \times 200 \times 220$
Linear absorption coefficient (mm^{-1})	12.09	11.99
Transmission factor range	0.41–0.52	0.18–0.26
Structure refinement:	Full-matrix, on $\sum\omega\cdot(\Delta F)^2$	
Anisotropic displacement parameter	Cs, Mn, and K	F
Number of refined parameters	11	7
Weighting scheme	$(\sigma_F^2 + 0.001\cdot F^2)^{-1}$	$(\sigma_F^2 + 0.0005\cdot F^2)^{-1}$
R for observed reflections	0.034	0.022
wR for observed reflections	0.035	0.028
wR for all unique reflections	0.062	0.052
Max. of $\|\Delta\|/\sigma$	< 0.001	< 0.001
Max. and min. of $\Delta\rho$ (e^- Å^{-3})	2.3 and -1.5	0.8 and -1.4

DISCUSSION

As discussed above the elpasolite type structure (cf. Fig. 1) of Cs_2KMnF_6 is formed by an array of alternating corner connected MnF_6 and KF_6 octahedra with 12-coordinated Cs atoms in the cuboctahedral interstices. As discussed above, an ordering of the distortions of the MnF_6 octahedra in the LT phase would lower the space group symmetry from cubic, for ideal elpasolites, to tetragonal for Cs_2KMnF_6. The magnitude of the distortions, as reflected by the unit-cell parameter ratio $a\sqrt{2}:c$ for the tetragonal LT phase, is 0.965. As discussed further below, a disorder of the distortion directions is apparently responsible for occurrence of the cubic symmetry of the HT phase, which seems likely due to their limited magnitudes. The prolate distortions of the MnF_6 octahedra in the LT phase, are typical for a d^4 ion (Jahn–Teller effects); two longer Mn–F bonding distances of 2.036(9) Å and four shorter distances of 1.860(6) Å. In the HT phase, all Mn–F distances become equal, 1.931(5) Å, by constraints due to the cubic space group symmetry. As has been shown (Norrestam (9)), the root harmonic mean square $(1/6\cdot\sum 1/r_1^2)^{1/2}$ estimate (rhms) of the radius of Mn^{3+} is constant and independent of the distortions contrary to average or root mean square estimates. From the standard value of 1.33 Å for the radius of the F^- ion and the bond lengths in the LT and HT phases, the rhms values for the Mn^{3+} ion become 0.58 and 0.60 Å, respectively, in good agreement with the average value 0.59(1) Å obtained by Norrestam (9).

The Mn^{3+} ions in the HT phase would give Jahn–Teller distortions of the coordination octahedra similar to those in the LT phase (see Fig. 2). The lack of observable Jahn–Teller distortions in the HT phase could be a static disorder of the axial distortions directions in the MnF_6 octahedra (see also

TABLE 2
Fractional Atomic Coordinates and Displacement Parameters with Estimated Standard Deviations (esds) for the Low-Temperature (LT) and High-Temperature (HT) Phases of Cs_2KMnF_6

Phase	Atom	x	y	z	u_{11}	u_{33}	U_{eq}
LT	Cs	1/2	0	1/4	0.0171(5)	0.0191(6)	0.0178(3)
	Mn	0	0	0	0.0039(13)	0.0074(19)	0.0051(9)
	K	0	0	1/2	0.018(2)	0.016(3)	0.0173(14)
	F1	0.2081(10)	0.2081(10)	0	—	—	0.023(2)
	F2	0	0	0.2197(10)	—	—	0.022(3)
HT	Cs	1/4	1/4	1/4	—	—	0.0283(14)
	Mn	0	0	0	—	—	0.0125(2)
	K	1/2	1/2	1/2	—	—	0.0251(5)
	F	0	0	0.2130(6)	0.0474(20)	0.031(3)	0.0417(14)

Note. Space group symmetry constraints on the displacement parameters imply that $u_{22} = u_{11}$ and $u_{23} = u_{13} = u_{12} = 0$ in both phases. Furthermore, $u_{11} = u_{22} = u_{33}$ for the metal atoms in the *HT* phases

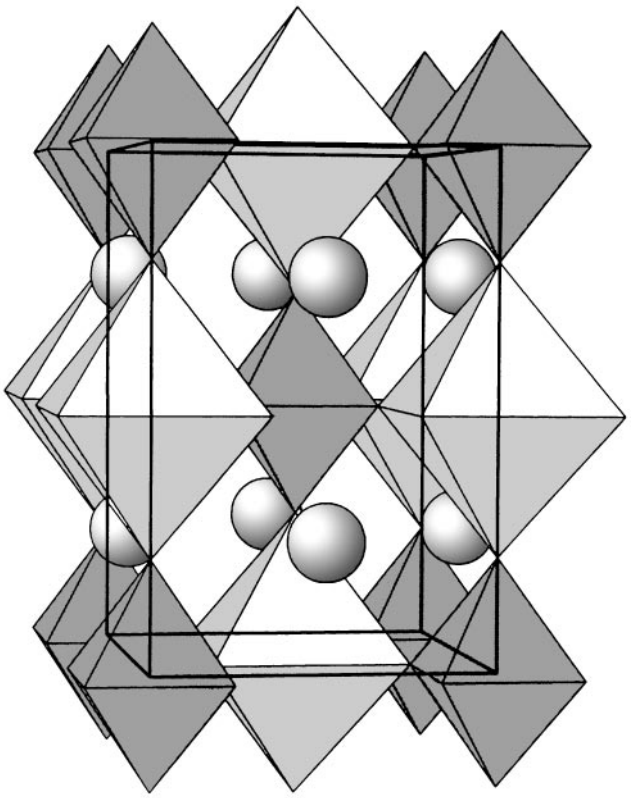

FIG. 1. Polyhedral representation of the cubic high-temperature (HT) phase of Cs_2KMnF_6 as viewed approximately along [1 0 0]. The origin is at the lower left corner, with [0 1 0] horizontal and [0 0 1] vertical. The MnF_6 and KF_6 polyhedra are represented by dark and light octahedra, respectively. For clarity, no coordination polyhedra are drawn around the Cs positions, which are shown as spheres.

Massa (10)). In such a case, the bond distances around Mn^{3+} will become a weighted average value between the two long and the four short Mn–F bonds. It could also be due to a dynamic Jahn–Teller effect. Both of these alternative explanations should i.a. lead to high values of the thermal displacement factors of the F^- atoms in the HT phase. The displacement parameters of the fluorine atoms in the HT phase are also approximately twice as large as those in the LT phase (0.022 and 0.042 $Å^2$, respectively). This fact supports the explanations given above for the lack of observable distortions in the HT phase.

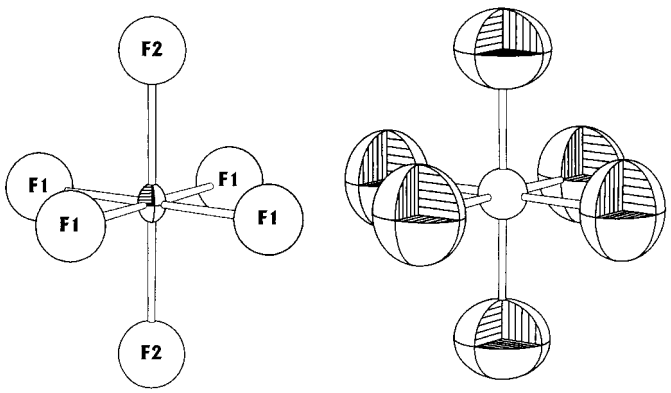

FIG. 2. The octahedral coordination around the Mn^{3+} ions. The atoms are represented by their 97% probability ellipsoids estimated from the refined thermal displacement parameters. The smaller isotropic displacements (left) in the LT phase and the higher anistropic displacements (right) in the HT phase are consistent with a static and/or dynamic disorder in the HT phase.

TABLE 3
Bond Distances with esds in the Low-Temperature (LT) and High-Temperature (HT) Phases of Cs_2KMnF_6

Phase	Atoms	Multiplicity	Distance (Å)
LT	Cs–F1	8	3.238(4)
	F2	4	3.172(1)
	Mn–F1	4	1.860(6)
	F2	2	2.034(9)
	K–F1	4	2.609(6)
	F2	2	2.595(9)
HT	Cs–F	12	3.223(1)
	Mn–F	6	1.931(5)
	K–F	6	2.602(5)

As seen in Table 3, the bond distances of the octahedrally coordinated potassium atom in the LT phase are $2 \times 2.597(9)$ and $4 \times 2.609(6)$ Å for K–F1 and K–F2, respectively. In the cubic HT phase the six K–F distances are all 2.602(5) Å. In the LT phase, the bonding distances to the 12-coordinated Cs atoms are $8 \times 3.240(4)$ and $4 \times 3.172(1)$ Å for Cs–F1 and Cs–F2, respectively. For the HT phase the Cs–F distances are $12 \times 3.223(1)$ Å.

Bond valence sums (bvs), using parameters from Brown and Altermatt (11) and Brese and O'Keeffe (12), for the LT and HT phases have been calculated and are shown in Table 4. The estimated bvs values for the LT and HT phases show a significant decrease for the manganese atom, from

TABLE 4
Estimated Bond Valence Sums (bvs) for the Low-Temperature (LT) and High-Temperature (HT) Phases of Cs_2KMnF_6

Phase	Atom	bvs
LT	Cs	1.10
	Mn	3.06
	K	1.14
	F1	1.11
	F2	0.97
HT	Cs	1.07
	Mn	2.88
	K	1.15
	F	1.03

Note. The bvs values were calculated as the sum of contributions (11, 12) for distances out to 3.6 Å.

3.06 to 2.88, respectively. For the caesium, potassium, and fluorine atoms the change in bvs values between the two phases are not significant.

ACKNOWLEDGMENTS

The authors are indebted to the Swedish National Research Council for the financial support of the present research project. We are also grateful to Jekabs Grins for his help with the DSC measurements.

REFERENCES

1. S. Schneider and R. Hoppe, *Z. Anorg. Allg. Chem.* **276,** 268 (1970).
2. K. Knox, *Acta Crystallogr. Sect. A* **16,** 45 (1963).
3. B. G. Hyde and S. Andersson, "Inorganic Crystal Structures." Wiley, New York, 1989.
4. R. D. Shannon, *Acta Crystallogr. Sect. A* **32,** 751 (1976).
5. "SHELXTL PC, release 4.1," Siemens Analytical X-Ray Instruments, Inc., 1990.
6. "International Tables for X-Ray Crystallography," Vol. IV. Birmingham, Kynoch Press, 1974.
7. A. L. Spek, "PLATON, Program for the Analysis of Molecular Geometry." University of Utrecht, 1990.
8. E. Dowty, "ATOMS," A Computer Program for Displaying Atomic Structures. Copyright Dowty, 521 Hidden Valley Road Kingsport, TN 37663, 1989.
9. R. Norrestam, *Z. Krist.* **209,** 99 (1994).
10. W. Massa, *Z. Anorg. Allg. Chem.* **491,** 208 (1982).
11. I. D. Brown and D. Altermatt, *Acta Crystallogr. Sect. B* **41,** 244 (1985).
12. N. E. Brese and M. O'Keeffe, *Acta Crystallogr. Sect. B* **47,** 192 (1991).